RESEARCH PAPERS
FACULTY OF MATERIALS SCIENCE AND TECHNOLOGY IN TRNAVA
SLOVAK UNIVERSITY OF TECHNOLOGY IN BRATISLAVA

2013 Special Number

COMPARISON OF OXIDATION RESISTANCE OF TiAlN MONOLAYER COATING AND ITS nACo3 NANOSTRUCTURED VERSION

Martin SAHUL, Paulína ZACKOVÁ, Ľubomír ČAPLOVIČ,
Kristián ŠALGÓ, Jana BOHOVIČOVÁ, Jozef SONDOR

ABSTRACT

The contribution deals with comparison of oxidation resistance of classical TiAlN monolayer coating and its advanced high hard nanostructured and multilayered nACo3 version at elevated temperatures. Both coatings were deposited onto AISI M36 high speed steel using unique LAteral Rotating Cathodes process (LARC®). "In – situ" X-Ray diffraction analysis was employed for determination of the beginning of oxides creation and phase detection at different heating temperatures. Scanning electron microscopy fitted with EDX analysis was used for observation of fracture areas and measurements of coatings and oxide layers thicknesses as well. Determination of chemical composition of coatings surfaces and elemental linescans through the coatings and oxide layers were performed using EDX analysis. All measurements of these coatings were carried out not only before but also after the thermal annealing.

KEY WORDS

TiAlN, nACo3, LARC®, In – Situ XRD analysis, SEM, LSM

INTRODUCTION

Nowadays, thin wear resistant hard coatings are widely applied on cutting and forming tools to improve their lifetime and performance, enhance productivity, and enable some new engineering applications as well. Hard coating deposition has now become a routine processing step in tools industry. Currently, a wide range of PVD hard coatings are available for a variety of applications [1, 2]. Due to the increasing lifetime and the cutting speed, the nanocomposite coatings are pushing the machining technology towards new horizons [3]. The study of TiAlN based coatings has deserved special attention. TiAlN is shown to have an excellent property in high speed cutting performance, such as oxidation resistance, mainly

Martin SAHUL, Paulína ZACKOVÁ, Ľubomír ČAPLOVIČ, Kristián ŠALGÓ, Jana BOHOVIČOVÁ - Slovak University of Technology, Faculty of Materials Science and Technology, Institute of Materials Science, J. Bottu 25, 917 24 Trnava, Slovakia, martin.sahul@stuba.sk, paulina.zackova@stuba.sk, lubomir.caplovic@stuba.sk, kristian.salgo@stuba.sk, jana.bohovicova@stuba.sk
Jozef SONDOR - LISS, a.s., Dopravní 2603, 756 61 Rožnov pod Radhoštěm, Czech Republic
j.sondor@liss.cz

because Al_2O_3 is formed on the interface between tool and work pieces at high cutting speeds [4]. Ti atoms are partly replaced by Al atoms in TiN, from this reason the hardness of TiAlN increases [1, 2, 3]. Nanostructured nACo3 coating consists of nanocrystallic grains with average size of 3 nm that are embedded in amorphous Si_3N_4 matrix. This coating offers higher hardness, oxidation resistance and lower thermal conductivity in comparison with TiAlN monolayer coating [5, 6]. During nACo3 nanocomposite PVD deposition, the TiAlN or TiN nanocrystals are dispersed in the growing amorphous Si_3N_4 matrix and the growth of nanocrystals is limited. When the external pressure is applied, the dislocations are motion – impeded by amorphous parts [7, 8], the hardness and toughness of the nACo3 coating are increased. With the increase of the silicon content in the nACo3 nanocomposite coating, the crystal size decreased. When the Si content is increased to 6.0 %, the coating exhibits a super hardness as well as an excellent fracture hardness and adhesion strength [9]. Small amount of Si increases the mechanical property of TiAlN coating, on the contrary, an excess Si decreases it, because the excessive Si forms a weak phase.

EXPERIMENTAL PROCEDURE

TiAlN monolayer coating and its nanocrystallic version that is called nACo3 were deposited by a PLATIT π80 lateral rotating cathodes arc system onto M36 high speed steel substrate. This steel is very suitable for production of tools that are designated to use in application of turning, milling and drilling hard machinable and high strength materials. The chemical composition of this steel is given in table 1.

CHEMICAL COMPOSITION OF AISI M36 HIGH SPEED STEEL Table 1

Chemical composition of AISI M36 HSS [wt. %]									
C	**Si**	**Mn**	**P**	**S**	**Co**	**Mo**	**Cr**	**V**	**W**
0.90	0.45	0.45	0.035	0.035	7.50	5.00	4.00	1.90	5.50

The PLATIT π80 deposition unit consists of two lateral rotating elemental cathodes, Ti (or Cr) and Al, and a rotating carrousel sample holder. This system has two major advantages over the conventional planar vacuum arc deposition systems. The first advantage comes from the unique lateral cathode rotation, which results in a maximum effective cathode surface and longer cathode lifetime. The second advantage comes from the Virtual Shutter function, which makes it possible for in situ cathode cleaning before coating deposition without plasma interruption. This feature results in superior adhesion strength and smooth surface of the as deposited coatings. Coatings were fabricated at LISS, a.s. Company in Rožnov pod Radhoštěm, Czech Republic. Coatings deposition was carried out in a flowing pure nitrogen atmosphere under a working pressure of 1.5 Pa. Ti/Al cylindrical target with Ti:Al atomic ratio of 1:1 was performed for evaporation of TiAlN coating. The second Al/Si cathode was employed during the deposition of nACo3 coating. Mirror polished M36 HSS disks with diameter of 10 mm were used as base materials. Before loading into the deposition chamber, these substrates were ultrasonically cleaned in a series of alkaline solutions. Next, they were washed with deionized water, blown dried by nitrogen gas and further dried in an oven at 100 °C. The pre cleaned substrates were then mounted on the carrousel substrate holder that rotates at a speed of 12 rpm during deposition. Prior to deposition, the substrates were bombarded by high energy ions to remove any traces of surface contamination and the native oxide layer. During deposition, a negative DC bias of−70 V was applied to the substrates and the deposition temperature was controlled at around 480 °C. Oxidation resistance and phase transformations that could occur inside these coatings during the heating process were studied using PANalytical Empyrean diffractometer that is fitted with PIXcel^{3D} detector and Anton

Paar DHS 1100 heating chamber. Parameters of XRD analysis were chosen with respect to coatings thicknesses (from 3 to 4 μm). From this reason, the Grazing Incidence XRD was performed due to suppress diffraction peaks achieved from the base material. Co anode with wavelength of 0.178897 nm was used as a source of radiation. These parameters were utilized during the analysis: U = 40 kV, I = 30 mA and step size of 0.01°/ 20 s. The specimens were heated up with heating rate of 30 K/min^{-1} and dwell time on each temperature stage was 10 min. Fracture areas of samples before and after thermal annealing were observed with high resolution field emission gun JEOL JSM 7600 F scanning electron microscope. All specimens were cleaned in acetone using ultrasonic energy before the observation. Specimens were observed in regime of backscattered electrons. Parameters of observation were: U = 20 keV, I = 2 nA and WD = 15 mm. The chemical composition of coatings surfaces were detected with X-Max 50 mm^2 EDX SDD detector. The elemental linescans through the coatings and oxide layers were achieved using the same detector as well.

RESULTS AND DISCUSSION

XRD patterns of TiAlN and nACo3 coatings achieved before and during the annealing process are documented in Fig. 1 a) and b). The structure of as deposited TiAlN mono coating consists of $TiAlN_2$ phase that is characterized with cubic unit cell with lattice parameter of 4.19 Å. The diffraction peak at the value of Bragg angle of 102° could be considered as a contribution of base material (ferrite) to the whole diffraction pattern. Diffraction peaks of TiN adhesion layer appears at Bragg angles of 50°, 40°, 100° and 124°. The phase transformation from ferrite to austenite occurred at the temperature of 900°C. The beginning of oxides layers formation was recorded at the temperature of 900°C as well. Above this temperature, the Al_2O_3 and TiO_2 oxides were detected.

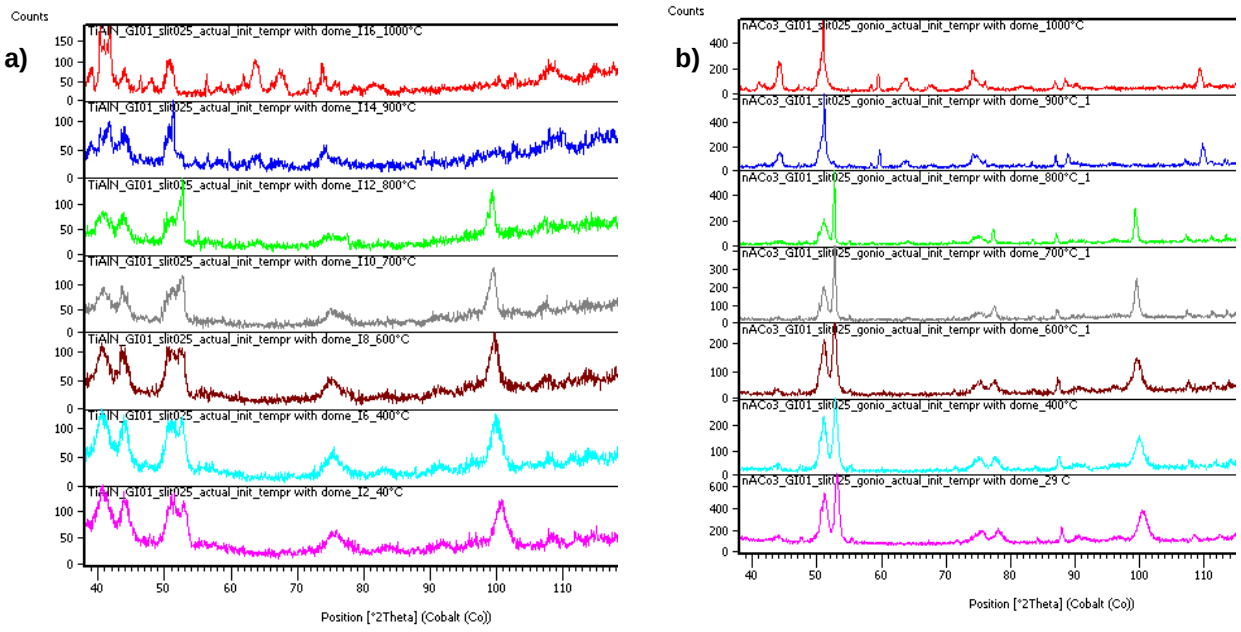

Fig. 1 *Diffraction patterns of a) TiAlN coating at elevated temperatures, b) nACo3 coating at elevated temperature*

The structure of nACo3 coating consists from $TiAlN_2$ phase before the thermal heating. The presence of amorphous Si_3N_4 matrix could not be detected due to its amorphous nature. The structure was stable until the temperature of 800 °C. The creation of first oxides was

observed at the temperature of 800 °C. Slight diffractions of Fe correspond to the contribution of substrate to the total diffraction pattern of the coating. TiO_2, SiO_2 and Al_2O_3 are the mainly oxides that were detected.

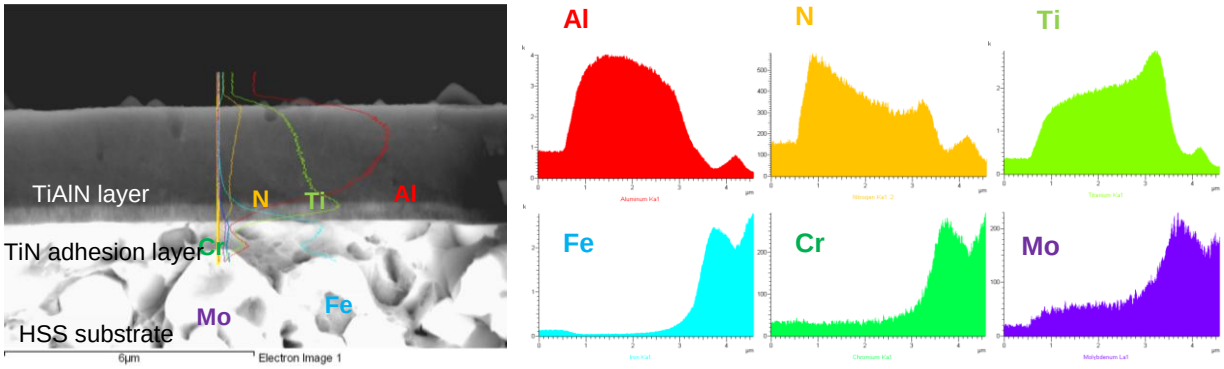

Fig. 2 *Fracture area of TiAlN coating before thermal heating and its chemical composition through the coating*

Structure of TiAlN fracture area monolayer before thermal annealing is given in Fig. 2. The presence of microparticles on the coating surface was proved. The thickness of TiAlN monolayer measured with SEM reached value of 2.76 µm. SEM also reveals that the monolayer consists of functional TiAlN layer and TiN adhesion layer. TiN interlayer was evaporated onto surface of base material due to improve the adhesion between TiAlN coating and AISI M36 substrate. The thickness of TiN adhesion layer was about 0.38 µm. The TiAlN coating is characterized by columnar crystal growth. Increase of Ti content from the top of the coating towards base material was documented by EDX linescan analysis across TiAlN coating – substrate interface. The intersection between the Ti and Al concentrations can be considered as the interface between TiAlN coating and TiN adhesion layer. Ti content reached its maximum value at the half of the adhesion layer.

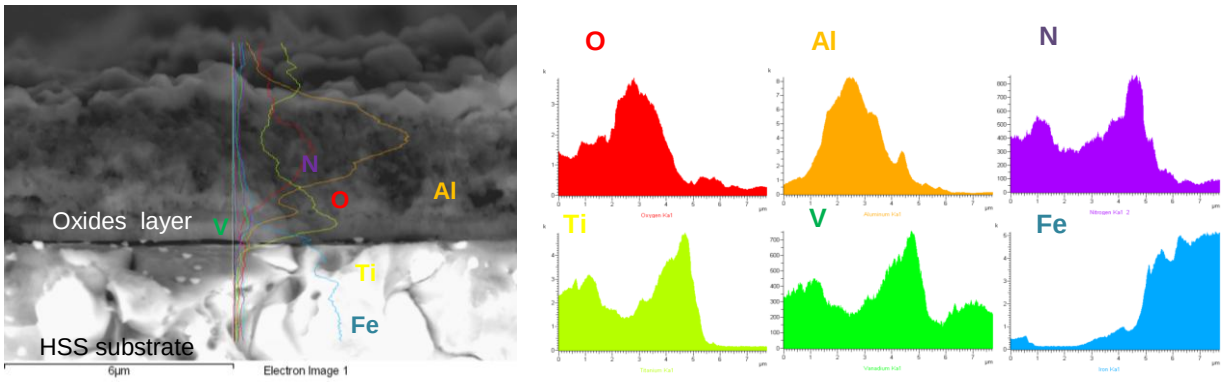

Fig. 3 *Fracture area of TiAlN coating after thermal heating and its chemical composition through the coating*

Structure of TiAlN coating fracture area after the heating process at the temperature of 1000 °C is documented in Fig. 3. SEM micrograph confirmed the presence of oxide layers created on the coating surface and failure of adhesion between the coating and base material. In this case, the thickness of TiAlN layer increased from 2.76 µm to 4.00 µm. It is caused by the oxide layers formation. Fig. 3 illustrates the course of concentration change of chemical elements across the TiAlN coating - base material interface after the oxidation process. Oxide

layers presented on the coating surface were mainly created from Al_2O_3 oxide. Diffusion of Vanadium from the substrate to TiN adhesion layer occurred. It assumed that the Vanadium substituted Ti atoms and caused the increasing of TiN adhesion layer lattice parameter. This could be a reason of lack of adhesion between the coating and substrate.

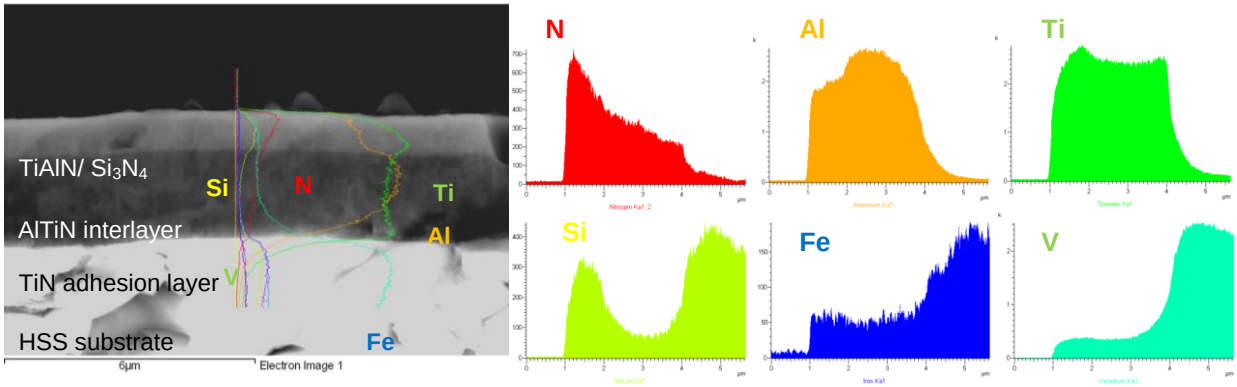

Fig. 4 *Fracture area of nACo3 coating before thermal heating and its chemical composition through the coating*

Fig. 4 illustrates the structure of nACo3 coating fracture area before the thermal heating process. The nACo3 coating belongs to the group of triple coatings. It means that, the coating consists from functional nanocrystallized TiAlN grains that are embedded in amorphous Si_3N_4 matrix. TiN adhesion layer was deposited onto substrate surface to improve adhesion between the coating and substrate. Connection between TiAlN/Si_3N_4 and TiN adhesion layer is realized using AlTiN interlayer. This interlayer improves the toughness of the coating. In this case, the columnar crystal growth was observed as well. The thickness of triple coating measured with SEM was approximately 3.13 µm. The thicknesses of individual layers are following: TiN adhesion layer is 0.14 µm, AlTiN interlayer is 2.03 µm and TiAlN/Si_3N_4 layer is 0.98 µm. The course of concentration change of elements across the interface of evaporated nACo3 coating to base material is documented in Fig. 4 as well. Constant growth of Si with its local maximum in the middle of the TiAlN/Si_3N_4 layer and constant decrease of N in the coating towards the interface were observed. Ti/Al ratio was changing through the functional coating and interlayer.

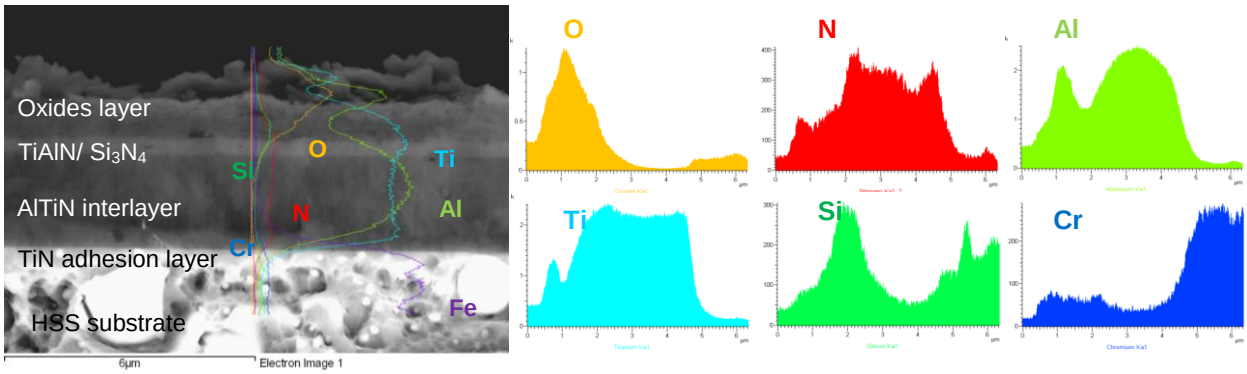

Fig. 5 *Fracture area of nACo3 coating after thermal heating and its chemical composition through the coating*

Structure of nACo3 coating fracture area after the heating process at the temperature of 1000 °C is documented in Fig. 5. The oxide layers on the coating surface were also observed. Based on EDX analysis we can assume that the oxides are dominantly created by Ti, Si and Al elements. The thickness of nACo3 coating increased from 3.13 µm to 3.49 µm.

CONCLUSIONS

The article dealt with the comparison of oxidation resistance of classical type of TiAlN monocoating and its new advanced nanocrystallic nACo3 version. “In situ” XRD analysis revealed the fact, the oxidation resistance of nACo3 coating is better than TiAlN. In addition, TiN adhesion layer lost its function after the thermal annealing of TiAlN coating. In the case of all coatings, the coating thicknesses increased after heating. It was caused by the formation of oxide layers. Formation of Al_2O_3 oxide layer on the surfaces of both coatings could lead to improve their wear resistance.

ACKNOWLEDGEMENTS

This publication is the result of the project implementation: CE for development and application of advanced diagnostic methods in processing of metallic and non-metallic materials, ITMS:26220120048, supported by the Research & Development Operational Programme funded by the ERDF. This research was supported by the grant project VEGA 1/1035/12.

REFERENCES

1. CHIM, Y. C., DING, X. Z., ZENG, X. T., ZHANG, S. 2009. Oxidation resistance of TiN, CrN, TiAlN and CrAlN coatings deposited by lateral rotating cathode arc. *Thin Solid Films*, **517**, pp. 4845 – 4849.
2. DING, X. Z., TAN, A. L. K., ZENG, X. T., WANG, C., YUE, T., SUN, C. Q. 2008. Corrosion resistance of CrAlN and TiAlN coatings deposited by lateral rotating cathode arc. *Thin Solid Films*, **516**, pp. 5716 – 5720.
3. PODGURSKY, V., NISUMAA, R., ADOBERG, E., SURZHENKOV, A., SIVITSKI, A., KULU, P. 2010. Comparative study of surface roughness and tribological behavior during running in period of hard coatings deposited by lateral rotating cathode arc. *Wear*, **268**, pp. 751 – 755.
4. DING, X. Z., ZENG, X. T., LIU, Y. C. 2011. Structure and properties of CrAlSiN Nanocomposite coatings deposited by lateral rotating cathode arc. *Thin Solid Films*, **519**, pp. 1894 – 1900.
5. PODGURSKY, V., ADOBERG, E., SURZHENKOV, A., KIMMARI, E., VILJUS, M., MIKLI, V., HARTELT, M., WÄSCHE, R., ŠÍMA, M., KULU, P. 2011. Dependence of the friction coefficient on roughness parameters during early stage fretting of (Al,Ti)N coated surfaces. *Wear*, **271**, pp. 853 – 858.
6. ARNDT, M., KACSICH, T. 2003. Performance of new AlTiN coatings in dry and high speed cutting. *Surface and Coatings Technology*, **163 – 164**, pp. 674 – 680.
7. MO, J. L., ZHU, M. H., LEYLAND, A., MATTHEWS, A. 2013. Impact wear and abrasion resistance of CrN, AlCrN and AlTiN PVD coatings. *Surface and Coatings Technology*, **215**, pp. 170 – 177.
8. CHANG, Y. Y., WANG, D. Y. 2007. Characterization of nanocrystalline AlTiN coatings synthesized by a cathodic arc deposition process. *Coatings and Surface Technology*, **201**, pp. 6699 – 6701.
9. LIU, A., DENG, J. X., CUI, H. B., CHEN, Y. Y., ZHAO, J. 2012. Friction and wear properties of TiN, TiAlN, AlTiN and CrAlN PVD nitride coatings. *Journal of Refractory Metals and Hard Materials*, **32**, pp. 82 – 88.